Free Radical Biology and Medicine 53 (2012) 730–741

Contents lists available at SciVerse ScienceDirect

Free Radical Biology and Medicine

journal homepage: www.elsevier.com/locate/freeradbiomed

Original Contribution

Activation of peroxisome proliferator-activated receptor-β/-δ (PPARβ/δ) prevents endothelial dysfunction in type 1 diabetic rats

Ana María Quintela [a], Rosario Jiménez [a], Manuel Gómez-Guzmán [a], María José Zarzuelo [a], Pilar Galindo [a], Manuel Sánchez [a], Félix Vargas [b], Ángel Cogolludo [c,d], Juan Tamargo [c], Francisco Pérez-Vizcaíno [c,d], Juan Duarte [a,*]

[a] Department of Pharmacology, School of Pharmacy, University of Granada, 18071 Granada, Spain
[b] Department of Physiology, School of Medicine, University of Granada, Granada, Spain
[c] Department of Pharmacology, School of Medicine, University Complutense of Madrid, Instituto de Investigación Sanitaria del Hospital Clínico San Carlos (IdISSC), Madrid, Spain
[d] Ciber Enfermedades Respiratorias (CIBERES), Madrid, Spain

ARTICLE INFO

Article history:
Received 10 January 2012
Received in revised form
30 May 2012
Accepted 31 May 2012
Available online 7 June 2012

Keywords:
PPARβ/δ
Diabetic rat
Endothelial dysfunction
NADPH oxidase

ABSTRACT

Endothelial dysfunction plays a key role in the pathogenesis of diabetic vascular disease. Herein, we have analyzed if the peroxisome proliferator-activated receptor-β/-δ (PPARβ/δ) agonist GW0742 exerts protective effects on endothelial function in type 1 diabetic rats. The rats were divided into 4 groups: control, control-treated (GW0742, 5 mg kg^{-1} day^{-1} for 5 weeks), diabetic (streptozotocin injection), and diabetic-treated. GW0742 administration in diabetic rats did not alter plasma glucose, systolic blood pressure, or heart rate, but reduced plasma triglyceride levels. The vasodilatation induced by acetylcholine was decreased in aortas from diabetic rats. GW0742 restored endothelial function, increasing eNOS phosphorylation. Superoxide production, NADPH oxidase activity, and mRNA expression of prepro endothelin-1, $p22^{phox}$, $p47^{phox}$, and NOX-1 were significantly higher in diabetic aortas, and GW0742 treatment prevented these changes. In addition, GW0742 prevented the endothelial dysfunction and the upregulation of prepro endothelin-1and $p47^{phox}$ after the in vitro incubation of aortic rings with high glucose and these effects were prevented by the PPARβ/δ antagonist GSK0660. PPARβ/δ activation restores endothelial function in type 1 diabetic rats. This effect seems to be related to an increase in nitric oxide bioavailability as a result of reduced NADPH oxidase-driven superoxide production and downregulation of prepro endothelin-1.

Introduction

Endothelial dysfunction plays a key role in the pathogenesis of diabetic vascular disease and is an independent risk factor of bad cardiovascular prognosis [1–3]. It has been suggested that elevated plasma glucose, LDL cholesterol, and reactive oxygen species (ROS) occurring in diabetes are causally involved in the development of this dysfunction [4,5]. Thus, endothelium- and nitric oxide (NO)-dependent relaxation may be impaired in diabetes by an excess generation of the ROS superoxide (O_2^-) which inactivates NO [2]. Increased levels of O_2^- are mainly attributable to NADPH oxidase activation within the vascular system [3,6–8], and/or to a decrease in antioxidant defense mechanisms, such as superoxide dismutase (SOD) [9,10].

The peroxisome proliferator-activated receptors (PPARs) PPARα, PPARβ/δ, and PPARγ are members of the nuclear hormone receptor superfamily. PPARs were initially believed to regulate genes involved only in lipid and glucose metabolism [11]. However, multiple evidence suggests that activation of PPARα or PPARγ may exert cardiovascular protective effects beyond their metabolic effects [12] including a reduction in blood pressure [13,14], reduced generation of ROS and proinflammatory mediators [14], and restoration of endothelial function [15–18]. Interestingly, PPARα and PPARγ are downregulated in diabetic states and this was associated with an increased expression of prepro endothelin-1 (ppET-1) mRNA which may trigger endothelial dysfunction [15]. In addition, PPAR-γ activators may prevent the deleterious ET-1-dependent proinflammatory vascular effects in hypertension [19].

Activation of the ubiquitously expressed PPARβ/δ also exhibits anti-inflammatory properties in the vessel wall by inhibiting the

Abbreviations: ACh, acetylcholine; CPT-1, carnitine palmitoyltransferase 1; DAPI, 4,6-diamidino-2-phenylindole dichlorohydrate; DHE, dihydroethidium; eNOS, endothelial NO synthase; EDHF, endothelium-derived hyperpolarizing factor; HR, heart rate; MCP-1, monocyte chemoattractant protein-1; MPO, myeloperoxidase; NO, nitric oxide; L-NAME, N^G-nitro-L-arginine methyl ester; PPARs, peroxisome proliferator-activated receptors; ppET-1, prepro endothelin-1; PDK4, pyruvate dehydrogenase kinase 4; ROS, reactive oxygen species; SHR, spontaneously hypertensive rats; STZ, streptozotocin; O_2^-, superoxide; SOD, superoxide dismutase; SBP, systolic blood pressure; VCAM-1, vascular cell adhesion molecule-1.

* Corresponding author. Fax: +34 958248264.
E-mail address: jmduarte@ugr.es (J. Duarte).

0891-5849/$ - see front matter © 2012 Elsevier Inc. All rights reserved.
http://dx.doi.org/10.1016/j.freeradbiomed.2012.05.045

expression of vascular cell adhesion molecule-1 (VCAM-1) and monocyte chemoattractant protein-1 (MCP-1) [20]. The PPARβ/δ agonist GW0742 reduced atherosclerosis in LDL receptor knockout ($LDLR^{-/-}$) mice [21], and substantially attenuated angiotensin II-accelerated atherosclerosis and the associated arterial inflammatory and atherosclerotic gene expression [22]. Moreover, GW0742 improved endothelial function in aortas from spontaneously hypertensive rats (SHR), which may be related to an interference with the intracellular signaling pathway induced by angiotensin II in the vascular wall [23]. Acute PPARβ/δ activation also protected the kidney against ischemia/reperfusion injury in diabetic rats [24], and chronic PPARβ/δ activation inhibited streptozotocin (STZ)-induced diabetic nephropathy through anti-inflammatory mechanisms [25], without altering blood glucose levels.

Notably, the potential protective effects on endothelial function of PPARβ/δ activation have not been tested in an animal model of type 1 diabetes. We hypothesized that the highly selective PPARβ/δ agonist GW0742 [26] would improve endothelial function in STZ-induced diabetic rats.

Material and methods

Animals and experimental groups

The experimental protocol followed the European Union guidelines for animal care and protection. Male Wistar rats, 280–320 g in weight, were maintained at a constant temperature (24 ± 1 °C), with a 12-h dark/light cycle and on standard rat chow. The animals were randomized to four experimental groups: untreated control group (vehicle, 1 ml of 1% methylcellulosa), untreated diabetic (vehicle), GW0742-treated control group ($5\ mg\ kg^{-1}$ per day, mixed in 1 ml of 1% methylcellulose, by oral gavage), and GW0742-treated diabetic group. Diabetic rats received a single injection via tail vein of STZ ($50\ mg\ kg^{-1}$ dissolved in a citrate buffer at pH, 4.5). Age-matched control rats were injected with the buffer alone. Three days after STZ injection, blood glucose levels were determined in 18 h fasted rats using an Accu-Check Aviva glucometer (Roche Diagnostics S.L., Barcelona, Spain). Rats with blood glucose levels of $200\ mg\ dl^{-1}$ or above [27] and polyuria were considered to be diabetic. GW0742 treatment was started 3 day after STZ or citrate buffer injection, and the treatment continued for 5 weeks. GW0742 is a highly potent and selective PPARβ/δ agonist with an EC50 value of 50 nmol/L for PPARβ/δ. The plasma concentration of GW0742 was not determined in the present study; however, it has been shown that mice treated with 1 and 10 mg/kg GW0742 for 4 weeks showed plasma concentrations of 440.7 and 2270 nmol/L, respectively [22], and LDLR-/- mice treated with 6 mg/kg for 16 weeks showed concentrations in the range of 805–1250 nmol/L [21]. Notably, the plasma concentration of the ligand at the 5 mg/kg dose would be expected to specifically activate PPAPβ without any cross-reactivity with other PPAR isoforms because the expected levels (< 2210 nmol/L) are bellow the reported EC50 values for murine PPARα (8900 nmol/L) and PPARγ ($> 10{,}000$ nmol/L) [21]. During the experimental periods rats had free access to tap water and chow. Body weight was measured every week. Systolic blood pressure (SBP) was measured every week in conscious rats by tail-cuff plethysmography [28].

Cardiac and renal weight indices, and plasma determinations

At the end of the experimental period, 18 h fasting animals were anesthetized with 2.5 ml/kg equitensin (ip) and blood was collected from the abdominal aorta. The heart and kidneys were excised, cleaned, and weighed. The atria and the right ventricle were then removed and the remaining left ventricle was weighed. The cardiac, left ventricular, right ventricular, and renal weight indices were calculated by dividing the heart, left ventricle, and kidney weight by the body weight. The Fulton index was calculated by dividing the right ventricular weight by the left ventricular plus septum weight. Plasma glucose, triglycerides, HDL, and total cholesterol concentrations were measured by colorimetric methods using Spinreact kits (Spinreact, S.A., Spain).

Vascular reactivity studies

Descending thoracic aortic rings (3 mm) and the third branch of the mesenteric artery (1.7–2 mm) were dissected from animals and were mounted in organ chambers and in a wire myograph (Model 610M, Danish Myo Technology, Aarhus, Denmark), respectively, filled with Krebs solution as previously described [29]. After equilibration, aortic rings were contracted by phenylephrine to obtain similar precontraction among groups (10^{-6} mol/L in control and both GW0742-treated groups and 3×10^{-7} mol/L in diabetic group) and concentration–relaxation response curves to acetylcholine (ACh) (10^{-9}–10^{-5} mol/L) were performed by cumulative addition in the absence or presence of the NO synthase (NOS) inhibitor N^G-nitro-L-arginine methyl ester (L-NAME, 10^{-4} mol/L). The concentration–relaxation response curves to sodium nitroprusside (10^{-9}–10^{-5} mol/L) were performed in the dark in rings without endothelium precontracted by 10^{-6} mol/L Phe. In some rings, a concentration–response curve to phenylephrine (10^{-9}–10^{-5} mol/L) was carried out by cumulative addition of the drug. The relaxant responses to ACh were also studied in intact-small mesenteric artery precontracted by phenylephrine (10^{-5} mol/L) in control or L-NAME-treated segments, or precontracted to KCl 80 mmol/L.

In another set of experiments, endothelium intact aortic rings were mounted in an organ bath, filled with normal Krebs solution. After testing the functionality of endothelium with ACh, rings were incubated in low (5 mmol/L) or high (44 mmol/L) glucose Krebs solution [30] for 6 h with or without PPARβ/δ agonists, GW0742 (10^{-6} mol/L) or L165041 (10^{-6} mol/L), and with or without prior (1 h) incubation with the PPARβ/δ antagonist, GSK0660 (10^{-6} mol/L). Then, after washing the preparation, the relaxant responses to ACh were studied in phenylephrine precontracted rings. Then, these rings were frozen (-80 °C) until quantitative RT-PCR analysis.

In situ detection of vascular ROS production

Unfixed thoracic aortic rings were cryopreserved (phosphate buffer solution 0.1 mol/L, PBS, plus 30% sucrose for 1–2 h), included in optimum cutting temperature compound medium (Tissue-Tek; Sakura Finetechnical, Tokyo, Japan), frozen (-80 °C), and 10-μm cross sections were obtained in a cryostat (Microm International Model HM500 OM). Sections were incubated for 30 min in Hepes-buffered solution containing dihydroethidium (DHE, 10^{-5} mol/L), counterstained with the nuclear stain 4,6-diamidino-2-phenylindole dichlorohydrate (DAPI, 3×10^{-7} mol/L), and in the following 24 h examined on a fluorescence microscope (Leica DM IRB, Wetzlar, Germany). Sections were photographed and ethidium and DAPI fluorescence was quantified using ImageJ (version 1.32j, NIH, http://rsb.info.nih/ij/). ROS production was estimated from the ratio of ethidium/DAPI fluorescence [28]. In preliminary experiments, before incubation with DHE, serial sections were treated with either the O_2^- scavenger tiron (10 μM), or pegylated superoxide dismutase (PEG-SOD, $250\ U\ ml^{-1}$) for 30 min at 37 °C.

NADPH oxidase activity

The lucigenin-enhanced chemiluminescence assay was used to determine NADPH oxidase activity in intact aortic rings, as previously described [4]. Aortic rings from all experimental groups were incubated for 30 min at 37 °C in Hepes-containing physiological salt solution (pH 7.4) of the following composition (in mmol/L): NaCl 119, Hepes 20, KCl 4.6, $MgSO_4$ 1, Na_2HPO_4 0.15, KH_2PO_4 0.4, $NaHCO_3$ 1, $CaCl_2$ 1.2, and glucose 5.5. Aortic production of O_2^- was stimulated by addition of NADPH (100 μmol/L). Rings were then placed in tubes containing physiological salt solution, with or without NADPH, and lucigenin was injected automatically at a final concentration of 5×10^{-6} mol/L to avoid known artifacts when used at a higher concentration. NADPH oxidase activity was determined by measuring luminescence over 200 s in a scintillation counter (Lumat LB 9507, Berthold, Germany) in 5-s intervals and was calculated by subtracting the basal values from those in the presence of NADPH. Vessels were then dried, and dry weight was determined. NADPH oxidase activity is expressed as relative luminescence units (RLU) per minute per milligram dry aortic tissue.

Immunohistochemical analysis

Unfixed thoracic aortic rings sections, included in optimum cutting temperature compound media, were incubated with a sodium citrate buffer (10 mM sodium citrate and 0,05% Tween 20, pH 6) at 95 °C for 20 min to retrieve the antigens. Endogenous peroxidase activity was inhibited with 1% H_2O_2 in PBS for 20 min. CD68 staining was performed using an anti-CD68 (EDI, 1:500 dilution; Santa Cruz Biotechnology, Santa Cruz, CA, USA) and InmunoCruz mouse ABC Staining System (Santa Cruz Biotechnology). Sections were counterstained with hematoxylin.

Myeloperoxidase activity assay

Myeloperoxidase (MPO) activity was measured in frozen aorta, homogenized, and centrifuged. Pellets were resuspended and subjected to three cycles of freezing and thawing prior to a final centrifugation step. The supernatants generated were assayed in triplicate for MPO activity using kinetic readings over 6 min at 460 nm (10 μl sample with 90 μl reaction buffer containing 50 mM potassium phosphate buffer, 0.167 mg ml^{-1} of odianisidine dihydrochloride and 0.0006% H_2O_2). The results are expressed as MPO units per gram of wet tissue.

Western blotting analysis

Aortic homogenates were run on a sodium dodecyl sulfate (SDS)–polyacrylamide gel electrophoresis. Proteins were transferred to polyvinylidene difluoride membranes (PVDF), incubated with primary monoclonal mouse anti-eNOS, rabbit antiphospho-eNOS (Ser 1177), anti-caveolin-1(Transduction Laboratories, San Diego, CA, USA), rabbit polyclonal antiphospho-caveolin-1 (Tyr14), monoclonal mouse anti-$p22^{phox}$, monoclonal mouse anti-NOX-2 (Santa Cruz Biotechnology, Santa Cruz, CA, USA), polyclonal rabbit anti-p47phox (Upstate Cell Signaling, Temecula, CA, USA), or polyclonal rabbit anti-NOX-1 (Novus Biologicals, Cambridge, UK) antibodies overnight and with the corresponding secondary peroxidase-conjugated antibodies. Antibody binding was detected by an ECL system (Amersham Pharmacia Biotech, Amersham, UK) and densitometric analysis was performed using Scion Image-Release Beta 4.02 software (http://www.scioncorp.com) [23,28]. Samples were reprobed for expression of smooth muscle α-actin.

Reverse transcriptase–polymerase chain reaction (RT-PCR) analysis

Total RNA was extracted from aorta by homogenization and converted to cDNA by standard methods. Polymerase chain reaction was performed with a Techgene thermocycler (Techne, Cambridge, UK). A quantitative real-time RT-PCR technique was used to analyze mRNA expression of PPARα, PPARγ, PPARβ/δ, and PPARβ/δ-target genes, such as PDK4 and CPT-1, caveolin-1, eNOS, $p22^{phox}$, $p47^{phox}$, NOX-1, NOX-4, and ppET-1. The sequences of the sense and antisense primers used for amplification are described in Table 1. Quantification was performed using the $\Delta\Delta C_t$ method. The housekeeping gene β-actin was used for internal normalization.

Drugs

GW0742 was purchased by Tocris Bioscence (Bristol, UK). All other drugs used were obtained from Sigma (Alcobendas, Madrid, Spain). All drugs and chemicals were dissolved in distilled deionized water.

Statistical analysis

Results are expressed as means ± SEM of measurements. Statistical differences were determined by one-way analysis followed by a post hoc Bonferroni's test for multiple comparisons. Individual cumulative concentration–response curves were fitted to a logistic equation. The maximal drug effect (E_{max}) and the negative log molar drug concentration producing 50% of the E_{max} ($-\log IC_{50}$ or $-\log EC_{50}$) were calculated from the fitted curves for each ring. $P < 0.05$ was considered significant.

Table 1
Oligonucleotides for real-time RT-PCR.

mRNA targets	Descriptions	Sense	Antisense
p47phox	p47phox subunit of NADPH oxidase	ATGACAGCCAGGTGAAGAAGC	CGATAGGTCTGAAGGCTGATGG
p22phox	p22phox subunit of NADPH oxidase	GCGGTGTGGACAGAAGTACC	CTTGGGTTTAGGCTCAATGG
caveolin-1	caveolin-1	TCTACAAGCCCAACAACAAGG	AGGAAAGAGAGGATGGCAAAG
eNOS	Endothelial nitric oxide synthase	ATGGATGAGCCAACTCAAGG	TGTCGTGTAATCGGTCTTGC
Actb	Beta actin	AATCGTGCGTGACATCAAAG	ATGCCACAGGATTCCATACC
PDK-4	pyruvate dehydrogenase kinase, isozyme 4	AGGTCGAGCTGTTCTCCCGCT	GCGGTCAGGCAGGATGTCAAT
CPT-1	carnitine palmitoyltransferase 1	TTCACTGTGACCCCAGACGGG	AATGGACCAGCCCCATGGAGA
NOX-1	NOX-1 subunit of NADPH oxidase	TCTTGCTGGTTGACACTTGC	TATGGGAGTGGGAATCTTGG
NOX-4	NOX-1 subunit of NADPH oxidase	ACAGTCCTGGCTTACCTTCG	TTCTGGGATCCTCATTCTGG
ppET-1	Prepro-endotelin-1	CTCGCTCTATGTAAGTCATGG	GCTCCTGCTCCTCCTGATG
PPAR-α	peroxisome proliferator-activated receptor alpha	TGTGACTGGTCAAGCTCAGG	CTTCCGGAACTCTCCTCTCC
PPAR-β/-δ	peroxisome proliferator-activated receptor beta/delta	CATTGAGCCCAAGTTCGAGT	GGTTGACCTGCAGATGGAAT
PPAR-γ	peroxisome proliferator-activated receptor gamma	AAGAACCATCCGATTGAAGC	CCAACAGCTTCTCCTTCTCG

Results

Effects of GW0742 on blood pressure, morphological variables, and plasma determinations

The plasma glucose and triglyceride levels were higher in diabetic rats while plasma HDL cholesterol levels, SBP, and HR were similar in diabetic compared to nondiabetic. Long-term GW0742 administration did not alter the levels of glucose, SBP, and HR, but reduced plasma triglyceride levels in diabetic rats and produced a not significant change in HDL cholesterol levels (Table 2).

Body weight was lower and heart weight/body weight, right ventricular weight/body weight, and kidney weight/body weight were higher in diabetic as compared to nondiabetic rats. The Fulton index, i.e., the right ventricular weight relative to left ventricular plus septum weight, an index of right ventricular hypertrophy was significantly increased in diabetes. Treatment with GW0742 lowered the right heart hypertrophy without affecting body weight, heart weight/body weight, and kidney weight/body weight (Table 3).

Effects of GW0742 on PPAR and PPARβ/δ-target genes in aorta

The gene expression of PPARα (Fig. 1A), PPARγ (Fig. 1B), and PPARβ/δ (Fig. 1C) was reduced, unchanged and increased, respectively, in the aorta from diabetic as compared with control rats. Chronic treatment with GW0742 increased mRNA of PPARβ/δ in diabetic rats without affecting the expression of PPARα and PPARγ. In diabetic control rings the mRNA levels of two well-known PPARβ/δ-target genes, pyruvate dehydrogenase kinase 4 (PDK4, Fig. 1D) and carnitine palmitoyltransferase 1 (CPT-1, Fig. 1E), were higher than in nondiabetic rats. As expected, the PPARβ/δ agonist significantly increased the expression of both genes in diabetic rats.

GW0742 prevents endothelial dysfunction in diabetic rats

Aortas from diabetic rats showed significant reduced endothelium-dependent vasodilator responses to ACh (considered as an index of endothelial function) as compared with aortas from the control group (Fig. 2A). The analysis of the concentration–response curve indicated that diabetes induced a change in the maximal relaxant response (E_{max} values were 69 ± 4 and $87 \pm 4\%$ in the diabetic and control groups, respectively, $P < 0.01$) without significant changes in the concentration of ACh required for half-maximal relaxation ($-\log IC_{50}$ values were 6.96 ± 0.18 and 7.29 ± 0.08 in the diabetic and control groups, respectively, $P > 0.05$). GW0742 produced a significant increase in the maximal relaxation induced by ACh in diabetic rats (E_{max} $86 \pm 3\%$, $P < 0.01$ vs diabetic group), being without effect in nondiabetic control rats (E_{max} $85 \pm 3\%$). The concentration–response curve to the α-adrenoceptor agonist phenylephrine showed an increased maximal response in the diabetic group compared with the control one (Fig. 2B, E_{max} 1.30 ± 0.14 vs 0.84 ± 0.10 g/g tissue, respectively, $P < 0.05$) without changes in the concentration of the vasoconstrictor required for half-maximal activation ($-\log EC_{50}$ values were 6.88 ± 0.06 and 6.81 ± 0.06 in the diabetic and control groups, respectively, $P > 0.05$). GW0742 treatment prevented the increase in the maximal vasoconstrictor response to phenylephrine in diabetic rats ($E_{max} = 0.92 \pm 0.13$ g/g tissue) without affecting control rats ($E_{max} = 0.82 \pm 0.09$ g/g tissue).

In mesenteric arteries precontracted with phenylephrine (10^{-5} mol/L) the concentration–relaxation curves to ACh were shifted to the right in arteries from diabetic rats compared to those from nondiabetic controls ($-\log IC_{50}$ 7.59 ± 0.12 vs 7.14 ± 0.11, respectively, $P < 0.05$), but the E_{max} was not different and complete relaxation of Phe-induced contraction was achieved in both groups. GW0742 significantly restored the ACh-induced in diabetic rats ($-\log IC_{50}$ 7.48 ± 0.07, $P < 0.05$) being without effect in nondiabetic controls ($-\log IC_{50}$ 7.58 ± 0.12, $P < 0.05$, Fig. 2C).

Role of endothelium-derived relaxing factors in the vascular effects of GW0742

In mesenteric arteries, the NOS inhibitor L-NAME (10^{-4} mol/L) produced a significant rightward shift of ACh-induced relaxation in both diabetic and control rats (data in Fig. 2D vs Fig. 2C). However, in the presence of this inhibitor, rings from diabetic animals were still significantly more resistant to relax in response to ACh and GW0742 treatment failed to restore this impaired

Table 2
Systolic blood pressure (SBP), heart rate (HR), and plasma determinations in all experimental groups.

Group	Control ($n=10$)	Control-treated ($n=8$)	Diabetic ($n=8$)	Diabetic-treated ($n=8$)
SBP initial (mm Hg)	157 ± 3	155 ± 4	164 ± 5	156 ± 3
SBP final (mm Hg)	158 ± 4	157 ± 5	153 ± 5	156 ± 4
HR initial (bpm)	429 ± 12	415 ± 16	445 ± 20	412 ± 11
HR final (bpm)	397 ± 16	410 ± 20	426 ± 34	426 ± 43
Cholesterol (mg/dl)	54.3 ± 3.4	58.2 ± 4.6	68.7 ± 4.2	75.2 ± 10
Triglycerides (mg/dl)	67.3 ± 5.7	43.4 ± 5.7	$103.9 \pm 14.7^{*}$	$68.1 \pm 11.8^{\ddagger}$
HDL (mg/dl)	41.7 ± 2.8	43.9 ± 3.6	38.4 ± 2.5	48.2 ± 3.9
Glucose (mg/dl)	115.8 ± 7.4	130.7 ± 6.0	$206.3 \pm 28.4^{\dagger}$	225.3 ± 23.6

Values are expressed as mean ± SEM of n rats. $^{*}P < 0.05$ and $^{\dagger}P < 0.01$ diabetic vs control; $^{\ddagger}P < 0.05$ GW0742-treated diabetic vs nontreated diabetic rats.

Table 3
Body and organ weights and cardiac and renal indices.

Groups	BW final (g)	HW (mg)	RVW (mg)	KW (mg)	HW/BW mg/g)	RVW/BW (mg/g)	RV/(LV+S) (mg/mg)	KW/BW(mg/g)
Control	333 ± 6	721 ± 17	164 ± 4	750 ± 15	2.17 ± 0.03	0.49 ± 0.01	0.296 ± 0.006	2.26 ± 0.03
Control-treated	317 ± 4	715 ± 12	158 ± 5	745 ± 12	2.25 ± 0.05	0.49 ± 0.01	0.291 ± 0.007	2.35 ± 0.06
Diabetic	$247 \pm 27^{\dagger}$	$603 \pm 55^{*}$	158 ± 19	$822 \pm 41^{*}$	$2.47 \pm 0.11^{*}$	$0.66 \pm 0.09^{*}$	$0.363 \pm 0.045^{*}$	$3.44 \pm 0.24^{\dagger}$
Diabetic-treated	254 ± 18	635 ± 33	138 ± 7	883 ± 28	2.54 ± 0.13	0.56 ± 0.04	$0.279 \pm 0.009^{\ddagger}$	3.59 ± 0.31

BW, body weight; HW, heart weight; RVW, right ventricle weight; KW, kidney weight, LV+S, left ventricle plus septum. Values are expressed as mean ± SEM of $n=8$–10 rats. $^{*}P < 0.05$ and $^{\dagger}P < 0.01$ diabetic vs control; $^{\ddagger}P < 0.05$ GW0742-treated diabetic vs nontreated diabetic rats.

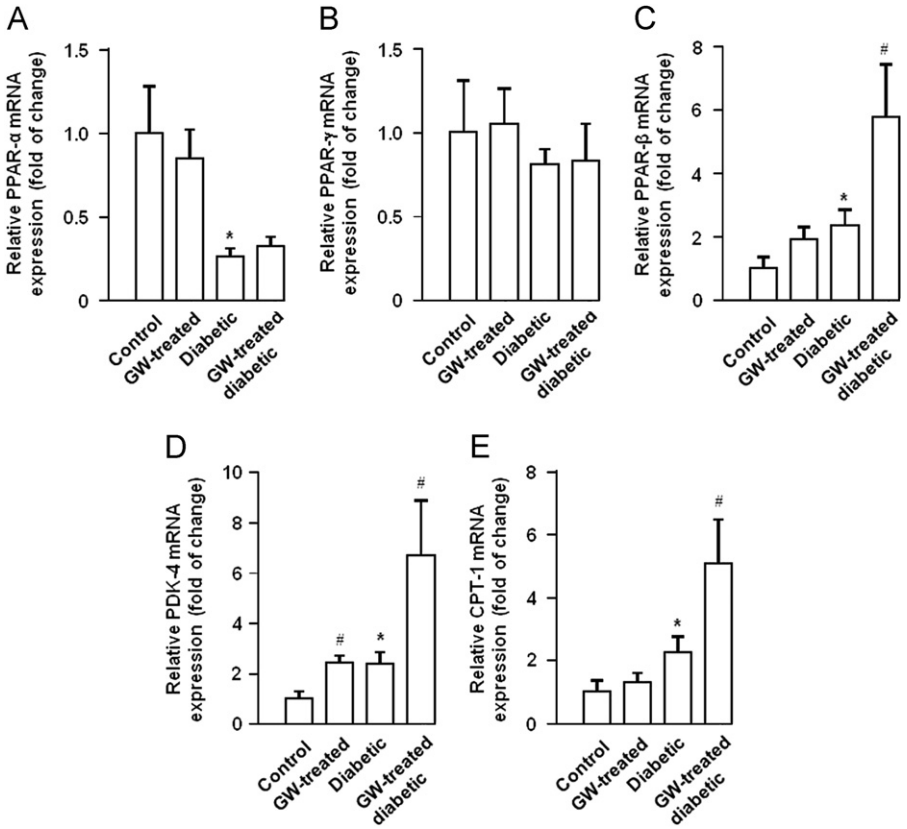

Fig. 1. Effects of GW0742 on PPAR and PPARβ/δ-target genes in aorta. mRNA levels of PPARα (A), PPARγ (B), PPARβ/δ (C), pyruvate deshydrogenase kinase 4 (PDK4) (D), and carnitine palmitoyltransferase 1 (CPT-1) (E) in nondiabetic and diabetic aortas. Results are shown as mean ± SEM, derived from 8 to 10 separate experiments. $^{*}P < 0.05$, diabetic vs control; $^{\#}P < 0.05$, GW0742-treated vs its respective untreated group.

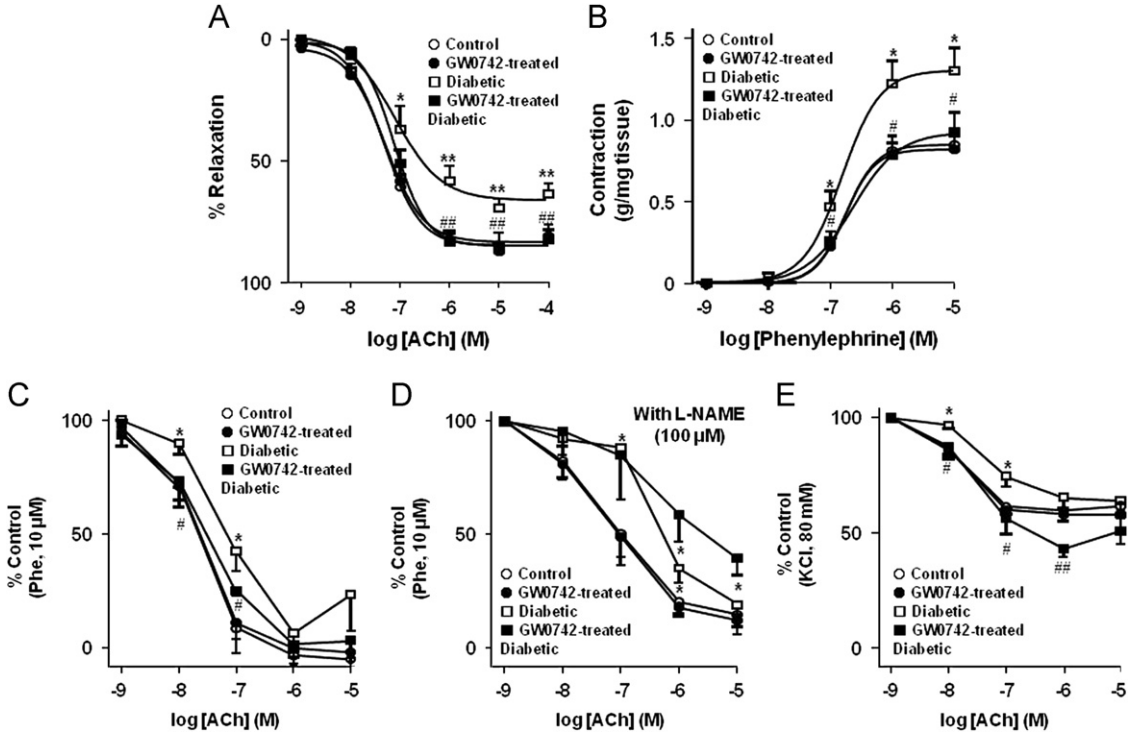

Fig. 2. Effects of GW0742 on endothelial function. Vascular relaxant responses induced by acetylcholine (ACh) in aortas (A) precontracted by phenylephrine (Phe), and contractile responses induced by Phe (B) in nondiabetic and diabetic rats. Vascular relaxant responses induced by ACh in mesenteric arteries precontracted by 10^{-5} mol/L Phe in the absence (C) and presence (D) of L-NAME (10^{-4} mol/L) and relaxant responses induced by ACh in mesenteric arteries precontracted by 80 mmol/L KCl (E) in nondiabetic and diabetic rats. Values are expressed as mean ± SEM (n=8–10 rings from different rats). $^{*}P < 0.05$ and $^{**}P < 0.01$ indicate, respectively, diabetic vs control. $^{\#}P < 0.05$ and $^{\#\#}P < 0.01$ indicate, respectively, GW0742-treated diabetic vs nontreated diabetic rats.

NO-independent relaxant response (Fig. 2D). When mesenteric arteries where precontracted by 80 mmol/L KCl, which depolarizes vascular smooth muscle and suppresses the effect of endothelium-derived hyperpolarizing factor (EDHF) [31], the E_{max} induced by ACh was strongly reduced as compared to Phe-precontracted rats (data in Fig. 2E vs Fig. 2C). This relaxation was abolished be L-NAME (data not shown). In KCl-stimulated arteries, the concentration–relaxant curve to ACh was also shifted to the right in diabetic as compared to control rats ($-\log IC_{50}$ 7.67 ± 0.06 vs 7.20 ± 0.14, respectively, $P < 0.01$), with similar E_{max} values (36.0 ± 7.1 vs 40.4 ± 2.4, respectively, $P > 0.01$) (Fig. 2E). Chronic GW0742 restored the impaired NO-mediated relaxant responses to ACh in KCl-precontracted mesenteric arteries from diabetic rats, increasing also the E_{max} ($-\log IC_{50}$ 7.41 ± 0.06 and E_{max} 57.2 ± 3.4).

In aorta, the relaxant response induced by ACh was fully inhibited by L-NAME in all experimental groups (Fig. 3A), showing that in this vessel ACh-induced relaxation in both control and diabetic rats was entirely dependent on endothelium-derived NO. Moreover, when the rings were incubated previously with the NO synthase inhibitor L-NAME, no differences were found among all experimental groups in the concentration–contractile response induced by phenylephrine in intact aortic rings (Fig. 3B). To analyze whether the impaired response to endothelial-derived NO is due to a reduced bioavailable NO or due to a defect in the signaling of NO in vascular smooth muscle, we analyzed the effects of nitroprusside, which directly activates soluble guanylyl cyclase in vascular smooth muscle, mimicking the effects of endogenous NO. The endothelium-independent vasodilator responses to nitroprusside were not different among groups (Fig. 3C). Endothelial NO synthase (eNOS, Fig. 3D and E) and caveolin-1 (Fig. 3F and G), an allosteric negative regulator of eNOS, gene, and protein expression in the aorta, were markedly higher in diabetic rats as compared with control animals. GW0742 did not affect the gene or protein expression of either eNOS (Fig. 3D and E) or caveolin-1 (Fig. 3F and G). We also found lower levels of phosphorylation of eNOS and caveolin-1 in diabetic animals as compared to control rats (Supplementary Fig. 1). GW0742 increased the levels of phosphorylation in protein in diabetic rats and also increased eNOS phosphorylation in control animals.

Effects of GW0742 on ROS and NADPH oxidase

To characterize and localize ROS levels within the vascular wall, ethidium red fluorescence was analyzed in sections of aorta incubated with DHE. Positive red nuclei could be observed in adventitial, medial, and endothelial cells from sections of aorta incubated with DHE (Fig. 4A). Staining was almost abolished by the O_2^- scavenger tiron and PEG-SOD (Fig. 4A). Nuclear red ethidium fluorescence was quantified and normalized to the blue fluorescence of the nuclear stain DAPI, allowing comparisons between different sections. Rings from diabetic rats showed marked increased staining in adventitial, medial, and endothelial cells as compared with WKY rats which was significantly reduced by GW0742 (Figs. 4A and B).

Since NADPH oxidase is the major source of ROS in the vascular wall, we investigated the effect of GW0742 on NADPH activity and gene expression of the main subunits in aorta from all experimental groups. NADPH oxidase activity was increased in aortic rings from diabetic as compared with control rats (Fig. 4C) and this was prevented by chronic treatment with GW0742. Significant mRNA overexpression of the NADPH oxidase subunits $p22^{phox}$ (Fig. 4D and H), $p47^{phox}$ (Fig. 4E, I), NOX-1 (Figs. 4F and J) was detected in rings from diabetic as compared to control rats without changes in NOX-4 mRNA (Fig. 4G) and NOX-2 protein

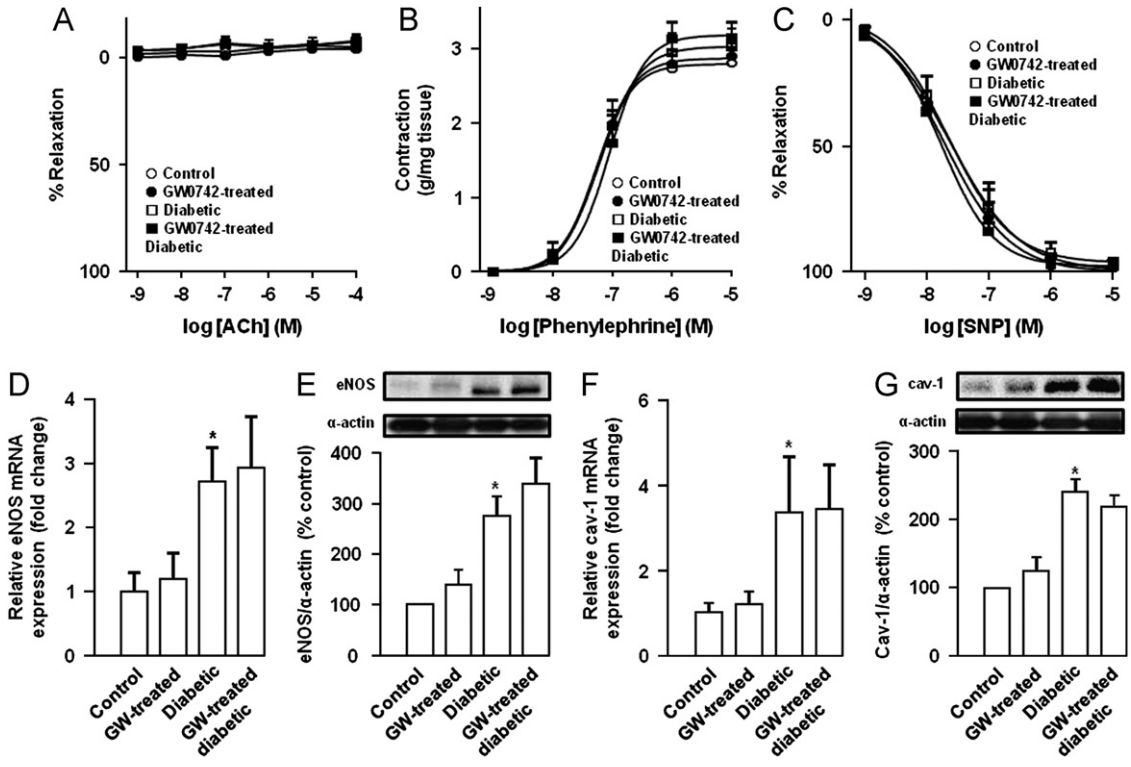

Fig. 3. Effects of GW0742 on the NO pathway in the rat aorta. Vascular relaxant responses induced by acetylcholine (ACh) (A) and contractile responses induced by phenylephrine (B) in the presence of L-NAME (10^{-4} mol/L). Relaxation induced by sodium nitroprusside (SNP) (B) in aortas precontracted by 10^{-6} mol/L Phe. Values are expressed as mean ± SEM (n=8–10 rings from different rats). Expression of eNOS (D and E) and caveolin-1 (F and G) at the level of mRNA by RT-PCR (D and F) and protein by Western blot (E and G) in control and diabetic rats. Results are shown as mean ± SEM, derived from 8 to 10 separate experiments. Data presented as densitometric values protein band normalized to the corresponding α-actin. Panels show representative bands (n=4–6). *$P < 0.05$, diabetic vs control.

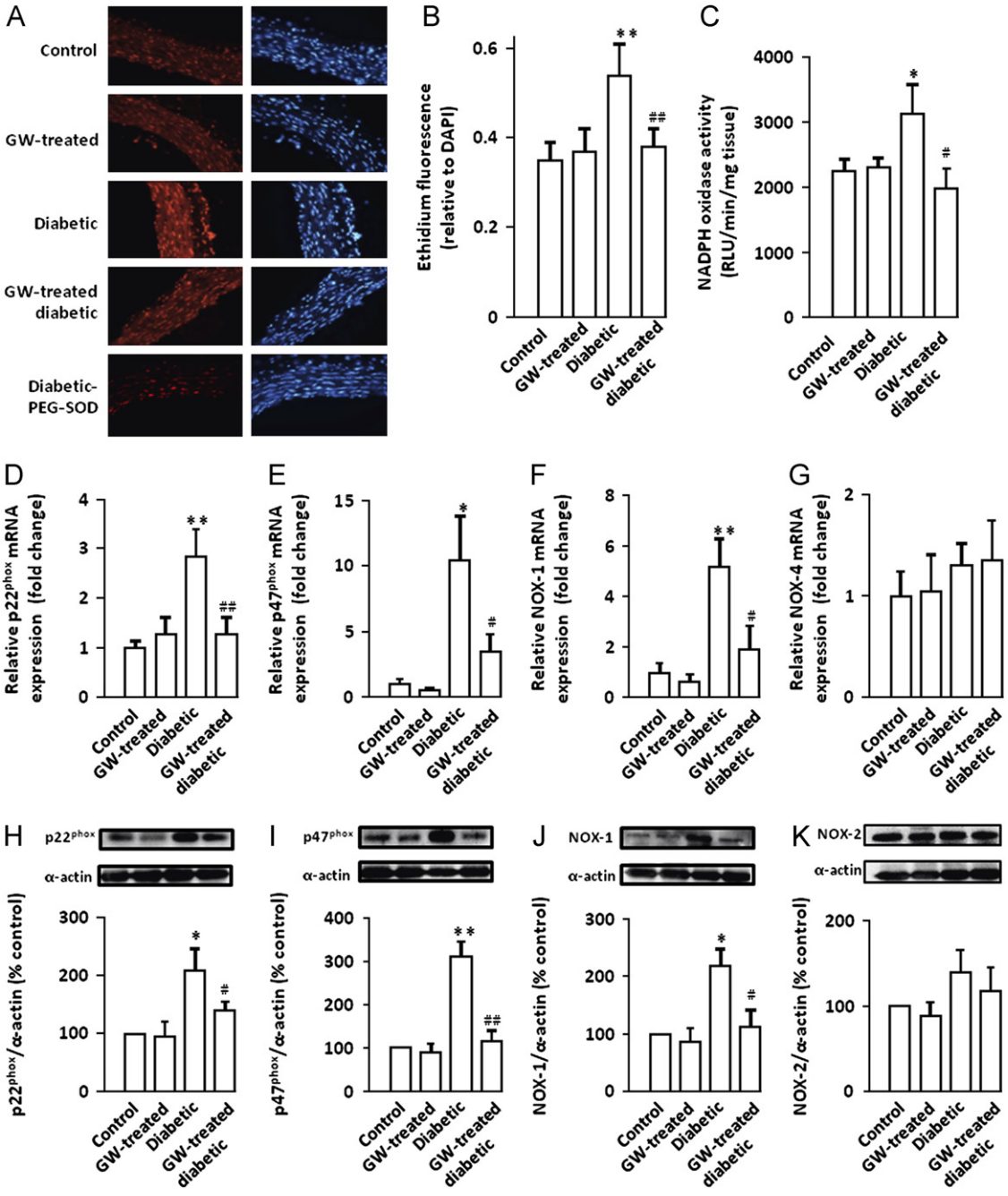

Fig. 4. Effects of GW0742 on ROS production and NADPH oxidase pathway. (A) Left pictures show arteries incubated in the presence of DHE which produces a red fluorescence when oxidized to ethidium by ROS. Right pictures show blue fluorescence of the nuclear stain DAPI ($\times 400$ magnification). Before incubation with DHE, serial sections were treated with pegylated superoxide dismutase (PEG-SOD, 250 U ml^{-1}) for 30 min. (B) Averaged values, mean $\pm$ SEM (n=8–10 rings from different rats), of the red ethidium fluorescence normalized to the blue DAPI fluorescence. NADPH oxidase activity measured by lucigenin-enhanced chemiluminescence (C) (n=6–10), and expression of NADPH oxidase subunits p22^{phox} (D, H) and p47^{phox} (E, I), NOX-1 (F, J), NOX-4 (G), and NOX-2 (K) at the level of mRNA by RT-PCR (D, E, F, and G) and protein by Western blot (H, I, J, and K) in nondiabetic and diabetic rats. Data presented as a ratio of arbitrary units of mRNA ($2^{-\Delta\Delta Ct}$) or densitometric protein band normalized to the corresponding α-actin. Results are shown as mean $\pm$ SEM, derived from 9 to 10 rings. * $P<0.05$ and ** $P<0.01$ indicate, respectively, diabetic vs control. # $P<0.05$ and ## $P<0.01$ indicate, respectively, GW0742-treated diabetic vs nontreated diabetic rats.

(Fig. 4K). Again, GW0742 treatment reduced mRNA overexpression of these subunits in diabetic rats.

Effects of GW0742 on macrophage infiltration

We analyzed the MPO activity in aortic tissue homogenates as a marker of neutrophil and macrophage infiltration. MPO activity was similar in all experimental groups (Supplementary Fig. 2A). Immunohistochemistry to CD68-positive macrophages also demonstrated no macrophages infiltration in aorta from all experimental groups (Supplementary Fig. 2B).

Effects on ET-1

ET-1 plays an important role in the endothelial dysfunction seen in diabetic state, and PPARs normalizes this dysfunction by improving the abnormal ET-1 system [17]. In order to determine if there is a relationship between PPARβ/δ and ET-1 in vascular wall, we investigated the expression of ppET-1 mRNA after

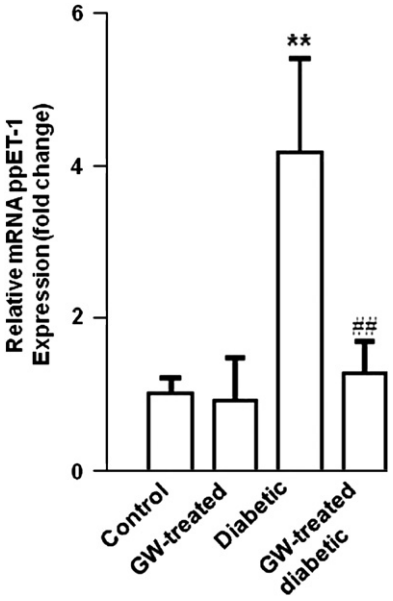

Fig. 5. Effect of GW0742 on mRNA expression of ppET-1. mRNA levels of ppET-in nondiabetic and diabetic aortas. Results are shown as mean ± SEM, derived from 8 to 10 separate experiments. ** $P < 0.01$, diabetic vs control. ## $P < 0.01$, GW0742-treated diabetic vs nontreated diabetic rats.

GW0742 treatment. The expression of ppET-1 mRNA was increased in diabetic rats and this increase was completely normalized by chronic GW0742 treatment (Fig. 5).

Role of the PPARβ/δ in endothelial dysfunction induced by High glucose in vitro

To further analyze the involvement PPARβ/δ activation on the protective effects of GW0742 in endothelial function a series of experiments were carried out in aortic rings incubated in vitro in low (5 mmol/L) or high (44 mmol/L) glucose medium for 6 h in the presence or the absence of GW0742 (1 μmol/L) and/or the PPARβ/δ antagonist GSK0660 (1 μmol/L). Aortas incubated with a high concentration of glucose exhibited a significantly weaker relaxation to ACh than aortas incubated under low glucose conditions (Fig. 6A). The same concentration of mannitol (5 mmol/L glucose + 39 mmol/L mannitol) had no effect on the endothelium-dependent relaxation to ACh (not shown), indicating that the high glucose damage was not due to a hyperosmotic effect. Coincubation with the PPARβ/δ ligand GW0742 had no effect on the relaxant responses to ACh in low glucose medium, but increased this relaxant response under high glucose conditions (Fig. 6A). Previous incubation with GSK0660 did not modify the relaxation to ACh under low or high glucose conditions, but prevented the increase induced by GW0742 in high glucose

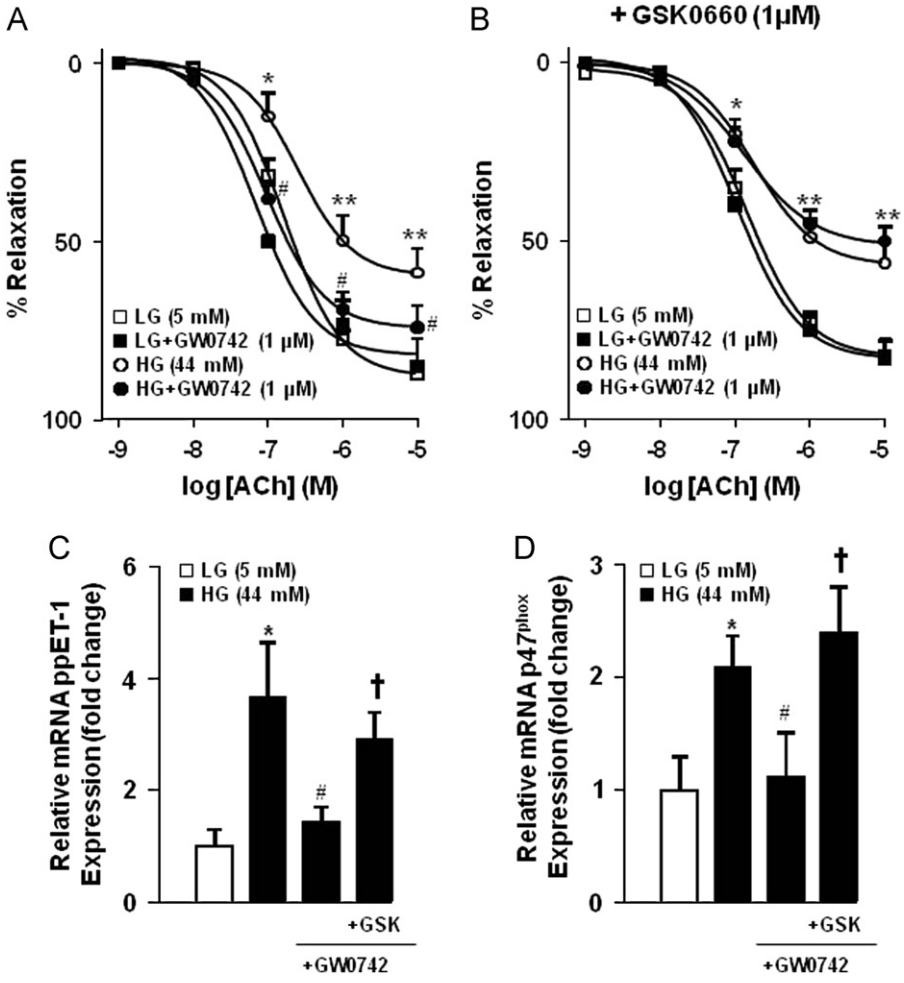

Fig. 6. Effects of GW0742 on endothelial dysfunction induced by high glucose in aortic rings in vitro. Vascular relaxant responses induced by acetylcholine (ACh) in aortic rings contracted by 10^{-5} mol/L phenylephrine after 6 h of incubation in vitro in low (5 mmol/L, LG) or high (44 mmol/L, HG) glucose medium with or without GW0742 (1 μmol/L) and in the absence (A) or the presence (B) of the PPARβ/δ antagonist GSK0660 (1 μmol/L). Effect of GW0742 on mRNA expression of ppET-1 (C) and and $p47^{phox}$ (D). Values are expressed as mean ± SEM ($n = 8$–10 rings from different rats). * $P < 0.05$ and ** $P < 0.01$ indicate, respectively, high vs low glucose. # $P < 0.05$, GW0742-treated high glucose vs nontreated high glucose arteries. † $P < 0.05$, GSK0660 plus GW0742-treated vs GW0742-treated.

medium (Fig. 6B). Moreover, the mRNA ppET-1 (Fig. 6C) and $p47^{phox}$ (Fig. 6D) upregulation induced by high glucose was also suppressed by GW0742, and this protective effect was abolished by coincubation with GSK0660.

Discussion

Our study provides the first evidence that chronic treatment with the highly selective PPARβ/δ agonist GW0742 restores the endothelium-dependent relaxation in aorta and small mesenteric arteries in type 1 diabetes. We chose the well established model of type 1 diabetes induced by STZ which shows: (1) an impairment of ACh-induced endothelium-dependent relaxation in several vascular beds [1,4,5,9,15,17,32,33], (2) reduced production of NO [6,34], and cGMP [1,17], (3) defective vascular response to EDHF in resistance arteries [31,35] (4) an increment in the generation of O_2^- [6,9,17,32–34], and (5) decreased expression of the mRNAs for PPAR-α and PPAR-γ and increased mRNA expression for PPARβ/δ in the aorta [15].

We previously found that GW0742 had a beneficial effect in endothelial function in SHR, which was related to improved glucose tolerance, increased HDL, and a direct effect in the vascular wall, reducing O_2^- production stimulated by angiotensin II [23]. In diabetic rats, the plasma lipids and glucose concentrations are increased [5,6,15,17,32],present results. In the present study GW0742 reduced plasma triglycerides without affecting plasma glucose and total cholesterol and with a borderline significant increase in HDL levels. Since, high triglycerides [36] and low HDL [37] are associated with impaired endothelial function, the changes induced by GW0742 in these parameters could account for the improved endothelial function in diabetic rats. However, most diabetic complications result from the increased plasma glucose and the increased generation of ROS, which may in turn lead to endothelial dysfunction [9,38]. Moreover, in our study, GW0742 also prevented both the endothelial dysfunction and the upregulation of ppET-1 and $p47^{phox}$ induced by high glucose in vitro, suggesting that both hyperglycemia and GW0742 exert direct effects in the vascular wall, independent of changes in lipid levels. In addition, these protective effects induced by GW0742 seem to be related to PPARβ/δ activation since they were suppressed by the PPRAβ antagonist GSK0660. Furthermore, we found that chronic GW0742 increased the vascular expression of two well-known PPARβ/δ-target genes, PDK4, which suppresses glucose oxidation by its inhibitory effects on the pyruvate deshydrogenase complex leading to an increase in fatty acid utilization, and CPT-1, which is involved in fatty acid β-oxidation [39]. The in vitro studies in isolated aortic rings are problematic because of the exceedingly high concentration of glucose used (44 mM), much higher than levels reached in vivo in STZ-diabetic rats. It is difficult to know to what extent the changes seen in vitro in arteries incubate in high glucose during a 6 h replicate those obtained in vivo in chronic diabetic animals.

Several studies from different laboratories have demonstrated that blood pressure is altered in animal models of diabetes. However, the results have not been consistent, since increase [16], decrease [40], and no change [41] in blood pressure have been described. The reasons for this discrepancy are not clear, but such variability is generally attributed to differences in the diabetogen used, the sex, species, and/or strain of the animals, the animal breeder, the duration of the hyperglycemia, and/or the blood pressure-measuring techniques and the experimental conditions. In the present study SBP was similar in STZ-diabetic rats than in the age-matched controls, and was unaltered by PPARβ/δ activation, an observation supported by previous reports showing that GW0742 treatment does not influence SBP in normotensive rats [42], but reduced blood pressure in hypertensive animals [23]. Pulmonary artery endothelial dysfunction, elevated pulmonary arterial pressure, and the subsequent right ventricular hypertrophy have been found in rats treated with STZ [33,43]. In the present study we also found right ventricular hypertrophy in diabetic rats, which was reduced by chronic GW0742 treatment, suggestive of improved pulmonary artery function. This is consistent with the therapeutic benefit of GW0742 in pulmonary arterial hypertension in a rat model of chronic hypoxia [42].

The contribution of vasoactive factors to the endothelial regulation of blood vessel tone varies depending on the vessel, age, sex, and animal species. In the rat aorta, NO is the major factor accounting for endothelium-dependent relaxation [44] as denoted by the full inhibitory action of L-NAME in this study. Thus, the diminished ACh-induced relaxation indicates an impaired agonist-induced NO bioactivity. Moreover, the increased contractile response to phenylephrine in the aorta from diabetic rats was suppressed by the presence of L-NAME, indicating that basal NO bioactivity was also impaired in the aorta from diabetic rats. Chronic GW0742 treatment prevented the altered responses to ACh and phenylephrine observed in diabetic aortas, indicating a protective role of this drug on both basal and agonist-induced NO bioactivity.

In mesenteric arteries both NO and EDHF contribute to endothelium-dependent relaxation while COX derived metabolites do not play any apparent role [2,35,45]. This is consistent with the inhibitory effects of the NOS inhibitor L-NAME and high K (standard pharmacological tools to inhibit NO and EDHF, respectively) in this study. ACh-induced relaxation is also reduced in mesenteric arteries from diabetic rats [46],presentresults, but the mechanisms involved are controversial. Thus, a selective impairment of the NO [45] or the EDHF [35] pathways or both simultaneously [47] has been reported. The present results, showing that in the presence of either L-NAME or high K the residual vasodilatations were still reduced in diabetes, are consistent with the view that both pathways are impaired. Chronic GW0742 enhanced ACh relaxation in the absence or in the presence of high K in mesenteric arteries. In contrast, this PPARβ/δ agonist had no effect after eNOS inihibition, indicating that it preserves the NO but does not affect the EDHF component of ACh-induced vasodilation.

Activation of endothelium- and NO-dependent pathways by ACh to induce relaxation requires: (1) Ca^{2+}-dependent activation of eNOS in endothelial cells leading to NO synthesis, (2) NO diffusion to the adjacent smooth muscle cells, (3) NO-induced activation of soluble guanylyl cyclase leading to cyclic GMP synthesis, and (4) activation of protein kinase G. All these steps in the signaling pathway of NO in systemic vessels have been reported to be impaired by high glucose in vitro and/or in type 1 and type 2 diabetes in vivo [3,34,48]. In the present study, the relaxant response to the activator of soluble guanylyl cyclase nitroprusside was similar in aorta from control and diabetic rats, treated or untreated with GW0742, indicating that alterations in the latter two steps noted above do not seem to contribute to endothelial dysfunction in diabetes or its prevention by GW0742. Thus, the functional changes observed in endothelium-dependent relaxation in the diabetic aorta should be attributed to an alteration in NO synthesis or its bioavailability. On the other hand, changes in the expression of eNOS in STZ-diabetic rats are controversial. Thus, increased, unchanged and decreased expression of eNOS in different systemic vessels has been reported [6,17,34,48]. Our data show that both mRNA and protein levels of eNOS were upregulated in aorta from diabetic animals compared with controls. However, the increase in its negative allosteric regulator caveolin-1 might collaborate to explain the reduced NO production found by others in diabetic aortic rings [6,34].

Again, GW0742 was unable to change eNOS and caveolin-1 expression. We also found lower levels of phosphorylation of eNOS and caveolin-1 in diabetic animals as compared to control rats. GW0742 increased the levels of phosphorylation in protein in diabetic rats and also increased eNOS phosphorylation in control animals. Increased eNOS phosphorylation would be involved in increased NO production. Moreover, activation of eNOS promotes Src-dependent caveolin-1-Tyr14 phosphorylation and eNOS/caveolin-1 binding, that is, eNOS feedback inhibition [49]. In our experiments, when the bioavailability of NO is limited, as occurs in diabetic rats, the levels of phospho-caveolin-1 are also lower as compared to control. GW0742, which increased NO in diabetic animals, also increased caveolin-1 phosphorylation.

A key mechanism of endothelial dysfunction involves the vascular production of ROS, particularly O_2^-, which reacts rapidly with and inactivates NO [50]. A considerable body of evidence suggests that the impairment of endothelium-dependent relaxation seen in diabetes involves inactivation of NO by O_2^- [2,3,10]. In aorta from diabetic rats incubated with DHE there was a marked increase in red fluorescence. DHE can react with O_2^- and other cellular oxidants to generate the two fluorescent products 2-hydroxyethidium and ethidium, respectively [51]. Whether the red fluorescence derived from 2-hydroxyethidium or ethidium cannot be fully ascertained. However, the inhibitory effect of the O_2^- scavengers tiron and PEG-SOD suggests that the primary source of oxidant stress is likely to be O_2^-. Chronic GW0742 abolished this increase in diabetic animals. The NADPH oxidase, a multienzymatic complex formed by $gp91^{phox}$ or its vascular homologous NOX-1 and NOX-4, rac, $p22^{phox}$, $p47^{phox}$, and $p67^{phox}$, is considered the major source of O_2^- in the vascular wall. Accumulating evidence suggests that vascular NADPH oxidase is the main source of increased ROS by high glucose in vitro [52], in animal models of diabetes [6,33] and in diabetic patients [7]. We found a marked increase in mRNA of $p22^{phox}$, $p47^{phox}$, and NOX-1, associated with a significant increase in the NADPH oxidase activity in aortas from diabetic rats, and also an increase in $p47^{phox}$ in the aortic ring incubated under high glucose conditions. GW0742 inhibited the upregulation of these subunits and the increase in NADPH oxidase activity in diabetic animals and had no effect in control rats. Dysregulation of eNOS activity under conditions associated with oxidative stress has also been related to eNOS uncoupling through loss of tetrahydrobiopterin [53]. Thus, it could be possible that the primary site of regulation is not the smooth muscle layer but the endothelium where NOX-2 in fact might also be dysregulated. However, we found no significant changes in NOX-2 protein expression in aorta from all experimental groups, excluding this possibility. Taken together the results suggest that the reduction of O_2^- derived from NADPH oxidase activity in vascular wall, and the subsequent prevention of NO inactivation, constitute the main mechanism involved in its protective effects on endothelial function.

Previous reports have involved ET-1 in the development of O_2^- production and endothelial dysfunction in diabetic rats. This is based on the following facts: (1) the plasma ET-1 levels are increased in STZ-induced diabetic rats, most likely due to an overexpression of the mRNA for ppET-1 [31,54], (2) the overproduction of ET-1 seen in STZ-induced diabetes results from the hyperglycemia, not from any increase in LDL cholesterol or triglyceride [40], (3) the increased expression of $p22^{phox}$ mRNA observed in STZ-induced diabetic rats is completely prevented by the chronic administration of J-104132 (a potent orally active mixed antagonist of ETA and ETB receptors) [32], and (4) prolonged treatment with ET-1 impairs endothelial function in the aorta both in nondiabetic rats and in rats with established STZ-induced diabetes, an effect that may be related to O_2^- generation [17,55]. In the present study, we also found an overexpression of the mRNA for ppET-1 in the STZ-induced diabetic aorta, which was suppressed by chronic GW0742. Downregulation of PPARα and PPARγ in the aorta contributes, through the ET-1 system, to the endothelial dysfunction seen in STZ-diabetic rats. In fact, chronic administration of bezafibrate (a PPARα agonist) to STZ-induced diabetic rats increased the expression PPARα and PPARγ, normalized both the mRNA for ppET-1 and the plasma concentration of ET-1, while improving endothelium-dependent relaxation [15]. Similarly, chronic pioglitazone (a PPARγ agonist) normalizes this dysfunction by improving the abnormal ET-1 system [17]. In our paper, GW0742, which increased PPARβ/δ, but not PPARα or PPARγ expression in aorta, also normalized ppET-1 expression, indicating that PPARβ/δ activation could also regulate vascular ET-1 production. Moreover, the upregulation of ppET-1 induced by high glucose in vitro was abolished by GW0742 in a PPARβ/δ-dependent manner, since this effect was also suppressed by the PPARβ/δ GSK0660. Thus, our results suggest that GW0742 normalizes diabetic endothelial dysfunction by improving the abnormal ET-1 system. However, other changes in diabetes, including increased local and systemic production of angiotensin, increased protein kinase C activity, decreased SOD, increased production of mitochondrial ROS, etc., have also been suggested to increase NADPH oxidase activity and/or ROS production. The potential contribution of these other factors and possible effects of GW0742 have not been established here.

In conclusion, our study demonstrates that in established STZ-diabetic rats, chronic PPARβ/δ treatment improves endothelium-dependent relaxation, essentially by preserving the NO-mediated component. This protective effect may be attributable to a decrease in the vascular ET-1 level, reducing oxidative stress by normalizing NADPH oxidase subunit expression. We believe that our findings should stimulate further interest in PPARβ/δ agonists as potential therapeutic drugs against diabetes-associated vascular disease.

Acknowledgments

This work was supported by Grants from Comisión Interministerial de Ciencia y Tecnología (SAF2011-28150, SAF2010-22066-C02-01 and -02) and by the Ministerio de Ciencia e Innovación, Instituto de Salud Carlos III (Red HERACLES RD06/0009), Spain. M.J.Z., P.G., and A.Q-P. are holders of studentships from Spanish Ministry of Science and Education.

Appendix A. Supporting information

Supplementary data associated with this article can be found in the online version at http://dx.doi.org/10.1016/j.freeradbiomed.2012.05.045.

References

[1] Kamata, K.; Miyata, N.; Kasuya, Y. Impairment of endothelium-dependent relaxation and changes in levels of cyclic GMP in aorta from streptozotocin-induced diabetic rats. *Br. J. Pharmacol* **97:**614–618; 1989.
[2] De Vriese, A. S.; Verbeuren, T. J.; Van de Voode, J.; Lameire, N. H.; Vanhoutte, P. M. Endothelial dysfunction in diabetes. *Br. J. Pharmacol.* **130:**963–974; 2000.
[3] Jay, D.; Hitomi, H.; Griedling, K. K. Oxidative stress and diabetic cardiovascular complications. *Free Radic. Biol. Med.* **40:**183–192; 2005.
[4] Kobayashi, T.; Kamata, K. Relationship among cholesterol, superoxide anion and endothelium-dependent relaxation in diabetic rats. *Eur. J. Pharmacol.* **367:**213–222; 1999.
[5] Kobayashi, T.; Matsumoto, T.; Kamata, K. Mechanisms underlying the chronic pravastatin treatment-induced improvement in the impaired

endothelium-dependent aortic relaxation seen in streptozotocin-induced diabetic rats. *Br. J. Pharmacol* **131:**231–238; 2000.
[6] Hink, U.; Li, H.; Mollnau, H.; Oelze, M.; Matheis, E.; Hartmann, M.; Skatchkov, M.; Thaiss, F.; Stahl, R. A.; Warnholtz, A.; Meinertz, T.; Griendling, K.; Harrison, D. G.; Forstermann, U.; Munzel, T. Mechanisms underlying endothelial dysfunction in diabetes mellitus. *Circ. Res.* **88:**E14–E22; 2001.
[7] Guzik, T. J.; Mussa, S.; Gastaldi, D.; Sadowski, J.; Ratnatunga, C.; Pillai, R.; Channon, K. M. Mechanisms of increased vascular superoxide production in human diabetes mellitus: role of NAD(P)H oxidase and endothelial nitric oxide synthase. *Circulation* **105:**1656–1662; 2002.
[8] Sonta, T.; Inoguchi, T.; Tsubouchi, H.; Sekiguchi, N.; Kobayashi, K.; Matsumoto, S.; Utsumi, H.; Nawata, H. Evidence for contribution of vascular NAD(P)H oxidase to increased oxidative stress in animal models of diabetes and obesity. *Free Radic. Biol. Med.* **37:**115–123; 2004.
[9] Kamata, K.; Kobayashi, T. Changes in superoxide dismutase mRNA expression by streptozotocin-induced diabetes. *Br. J. Pharmacol.* **119:**583–589; 1996.
[10] Spitaler, M. M.; Graier, W. F. Vascular targets of redox signaling in diabetes mellitus. *Diabetologia* **45:**476–494; 2002.
[11] Marx, N.; Duez, H.; Fruchart, J. C.; Staels, B. Peroxisome proliferator-activated receptors and atherogenesis: regulators of gene expression in vascular cells. *Circ. Res.* **94:**1168–1178; 2004.
[12] Leibovitz, E.; Schiffrin, E. L. PPAR activation: a new target for the treatment of hypertension. *J. Cardiovasc. Pharmacol.* **50:**120–125; 2007.
[13] Raji, A.; Seely, E. W.; Bekins, S. A.; Williams, G. H.; Simonson, D. C. Rosiglitazone improves insulin sensitivity and lowers blood pressure in hypertensive patients. *Diabetes Care* **26:**172–178; 2003.
[14] Diep, Q. N.; Amiri, F.; Touyz, R. M.; Cohn, J. S.; Endemann, D.; Neves, M. F.; Schiffrin, E. L. PPAR α activator effects on Ang II-induced vascular oxidative stress and inflammation. *Hypertension* **40:**866–871; 2002.
[15] Kanie, N.; Matsumoto, T.; Kobayashi, T.; Kamata, K. Relationship between peroxisome proliferator-activated receptors (PPAR alpha and PPAR gamma) and endothelium-dependent relaxation in streptozotocin-induced diabetic rats. *Br. J. Pharmacol.* **140:**23–32; 2003.
[16] Majithiya, J. B.; Paramar, A. N.; Balaraman, R. Pioglitazone, a PPARgamma agonist, restores endothelial function in aorta of streptozotocin-induced diabetic rats. *Cardiovasc. Res.* **66:**150–161; 2005.
[17] Matsumoto, T.; Noguchi, E.; Kobayashi, T.; Kamata, K. Mechanisms underlying the chronic pioglitazone treatment-induced improvement in the impaired endothelium-dependent relaxation seen in aortas from diabetic rats. *Free Radic. Biol. Med* **42:**993–1007; 2007.
[18] Olukman, M.; Sezer, E. D.; Ulker, S.; Sözmen, E. Y.; Cınar, G. M. Fenofibrate treatment enhances antioxidant status and attenuates endothelial dysfunction in streptozotocin-induced diabetic rats. *Exp. Diabetes Res.* **2010:**828531; 2010.
[19] Montezano, A. C.; Amiri, F.; Tostes, R. C.; Touyz, R. M.; Schiffrin, E. L. Inhibitory effects of PPAR-gamma on endothelin-1-induced inflammatory pathways in vascular smooth muscle cells from normotensive and hypertensive rats. *J. Am. Soc. Hypertens* **1:**150–160; 2007.
[20] Rival, Y.; Benéteau, N.; Taillandier, T.; Pezet, M.; Dupont-Passelaigue, E.; Patoiseau, J. F.; Junquéro, D.; Colpaert, F. C.; Delhon, A. PPARα and PPARδ activators inhibit cytokine-induced nuclear translocation of NF-κB and expression of VCAM-1 in EAhy926 endothelial cells. *Eur. J. Pharmacol.* **435:**143–151; 2002.
[21] Graham, T. L.; Mookherjee, C.; Suckling, K. E.; Palmer, C. N.; Patel, L. The PPARdelta agonist GW0742X reduces atherosclerosis in LDLR(-/-) mice. *Atherosclerosis* **181:**29–37; 2005.
[22] Takata, Y.; Liu, J.; Yin, F.; Collins, A. R.; Lyon, C. J.; Lee, C. H.; Atkins, A. R.; Downes, M.; Barish, G. D.; Evans, R. M.; Hsueh, W. A.; Tangirala, R. K. PPARdelta-mediated antiinflammatory mechanisms inhibit angiotensin II-accelerated atherosclerosis. *Proc. Natl. Acad. Sci. USA* **105:**4277–4282; 2008.
[23] Zarzuelo, M. J.; Jiménez, R.; Galindo, P.; Sánchez, M.; Nieto, A.; Romero, M.; Quintela, A. M.; López-Sepúlveda, R.; Gómez-Guzmán, M.; Bailón, E.; Rodríguez-Gómez, I.; Zarzuelo, A.; Gálvez, J.; Tamargo, J.; Pérez-Vizcaíno, F.; Duarte, J. Antihypertensive effects of peroxisome proliferator-activated receptor-β activation in spontaneously hypertensive rats. *Hypertension* **58:**733–743; 2011.
[24] Collino, M.; Benetti, E.; Miglio, G.; Castiglia, S.; Rosa, A. C.; Aragno, M.; Thiemermann, C.; Fantozzi, R. Peroxisome proliferator-activated receptor β/δ agonism protects the kidney against ischemia/reperfusion injury in diabetic rats. *Free Radic. Biol. Med.* **50:**345–353; 2011.
[25] Matsushita, Y.; Ogawa, D.; Wada, J.; Yamamoto, N.; Shikata, K.; Sato, C.; Tachibana, H.; Toyota, N.; Makino, H. Activation of peroxisome proliferator-activated receptor delta inhibits streptozotocin-induced diabetic nephropathy through anti-inflammatory mechanisms in mice. *Diabetes* **60:**960–968; 2011.
[26] Sznaidman, M. L.; Haffner, C. D.; Maloney, P. R.; Fivush, A.; Chao, E.; Goreham, D.; Sierra, M. L.; LeGrumelec, C.; Xu, H. E.; Montana, V. G.; Lambert, M. H.; Willson, T. M.; Oliver Jr W. R.; Sternbach, D. D. Novel selective small molecule agonists for peroxisome proliferator-activated receptor delta (PPARdelta)–synthesis and biological activity. *Bioorg. Med. Chem. Lett.* **13:**1517–1521; 2003.
[27] Camici, G. G.; Schiavoni, M.; Francia, P.; Bachschmid, M.; Martin-Padura, I.; Hersberger, M.; Tanner, F. C.; Pelicci, P.; Volpe, M.; Anversa, P.; Lüscher, T. F.; Cosentino, F. Genetic deletion of p66(Shc) adaptor protein prevents hyperglycemia-induced endothelial dysfunction and oxidative stress. *Proc. Natl. Acad. Sci. USA* **104:**5217–5222; 2007.
[28] Jiménez, R.; López-Sepúlveda, R.; Kadmiri, M.; Romero, M.; Vera, R.; Sánchez, M.; Vargas, F.; O'Valle, F.; Zarzuelo, A.; Dueñas, M.; Santos-Buelga, C.; Duarte, J. Polyphenols restore endothelial function in DOCA-salt hypertension: role of endothelin-1 and NADPH oxidase. *Free Radic. Biol. Med.* **43:**462–473; 2007.
[29] Gómez-Guzmán, M.; Jiménez, R.; Sánchez, M.; Romero, M.; O'Valle, F.; Lopez-Sepulveda, R.; Quintela, A. M.; Galindo, P.; Zarzuelo, M. J.; Bailón, E.; Delpón, E.; Perez-Vizcaino, F.; Duarte, J. Chronic (-)-epicatechin improves vascular oxidative and inflammatory status but not hypertension in chronic nitric oxide-deficient rats. *Br. J. Nutr.* **106:**1337–1348; 2011.
[30] Qian, L. B.; Wang, H. P.; Chen, Y.; Chen, F. X.; Ma, Y. Y.; Bruce, I. C.; Xia, Q. Luteolin reduces high glucose-mediated impairment of endothelium-dependent relaxation in rat aorta by reducing oxidative stress. *Pharmacol. Res.* **61:**281–287; 2010.
[31] Makino, A.; Ohuchi, K.; Kamata, K. Mechanisms underlying the attenuation of endothelium-dependent vasodilatation in the mesenteric arterial bed of the streptozotocin-induced diabetic rat. *Br. J. Pharmacol* **130:**549–556; 2000.
[32] Kanie, N.; Kamata, K. Effects of chronic administration of the novel endothelin antagonist J-101432 on endothelial dysfunction in streptozotocin-induced diabetic rat. *Br. J. Pharmacol* **135:**1935–1942; 2002.
[33] Lopez-Lopez, J. G.; Moral-Sanz, J.; Frazziano, G.; Gomez-Villalobos, M. J.; Flores-Hernandez, J.; Monjaraz, E.; Cogolludo, A.; Perez-Vizcaino, F. Diabetes induces pulmonary artery endothelial dysfunction by NADPH oxidase induction. *Am. J. Physiol. Lung Cell Mol. Physiol* **295:**L727–L732; 2008.
[34] Wendt, M. C.; Daiber, A.; Kleschyov, A. L.; Mülsch, A.; Sydow, K.; Schulz, E.; Chen, K.; Keaney Jr J. F.; Lassègue, B.; Walter, U.; Griendling, K. K.; Münzel, T. Differential effects of diabetes on the expression of the gp91phox homologues nox1 and nox4. *Free Radic. Biol. Med.* **39:**381–391; 2005.
[35] Wigg, S. J.; Tare, M.; Tonta, M. A.; O'Brien, R. C.; Meredith, I. T.; Parkington, H. C. Comparison of effects of diabetes mellitus on an EDHF-dependent and an EDHF-independent artery. *Am. J. Physiol. Heart Circ. Physiol* **281:**H232–H240; 2001.
[36] Kamata, K.; Yamashita, K. Insulin resistance and impaired endothelium-dependent renal vasodilatation in fructose-fed hypertensive rats. *Res. Commun. Mol. Pathol. Pharmacol* **103:**195–210; 1999.
[37] Van Linthout, S.; Spillmann, F.; Lorenz, M.; Meloni, M.; Jacobs, F.; Egorova, M.; Stangl, V.; De Geest, B.; Schultheiss, H. P.; Tschöpe, C. Vascular-protective effects of high-density lipoprotein include the downregulation of the angiotensin II type 1 receptor. *Hypertension* **53:**682–687; 2009.
[38] Takenouchi, Y.; Kobayashi, T.; Taguchi, K.; Matsumoto, T.; Kamata, K. Relationship among superoxide-related enzyme, PPARs, and endothelium-dependent relaxation in murine aortas previously organ-cultured in high-glucose conditions. *Can. J. Physiol. Pharmacol.* **88:**760–769; 2010.
[39] Tanaka, T.; Yamamoto, J.; Iwasaki, S.; Asaba, H.; Hamura, H.; Ikeda, Y.; Watanabe, M.; Magoori, K.; Ioka, R. X.; Tachibana, K.; Watanabe, Y.; Uchiyama, Y.; Sumi, K.; Iguchi, H.; Ito, S.; Doi, T.; Hamakubo, T.; Naito, M.; Auwerx, J.; Yanagisawa, M.; Kodama, T.; Sakai, J. Activation of peroxisome proliferator-activated receptor delta induces fatty acid beta-oxidation in skeletal muscle and attenuates metabolic syndrome. *Proc. Natl. Acad. Sci. USA* **100:**15924–15929; 2003.
[40] Makino, A.; Kamata, K. Time-course changes in plasma endothelin-1 and its effects on the mesenteric arterial bed in streptozotocin-induced diabetic rats. *Diabetes Obes. Metab* **2:**47–55; 2000.
[41] Tone, A.; Shikata, K.; Sasaki, M.; Ohga, S.; Yozai, K.; Nishishita, S.; Usui, H.; Nagase, R.; Ogawa, D.; Okada, S.; Shikata, Y.; Wada, J.; Makino, H. Erythromycin ameliorates renal injury via anti-inflammatory effects in experimental diabetic rats. *Diabetologia* **48:**2402–2411; 2005.
[42] Harrington, L. S.; Moreno, L.; Reed, A.; Wort, S. J.; Desvergne, B.; Garland, C.; Zhao, L.; Mitchell, J. A. The PPARbeta/delta agonist GW0742 relaxes pulmonary vessels and limits right heart hypertrophy in rats with hypoxia-induced pulmonary hypertension. *PLoS One* **5:**e9526; 2010.
[43] Al-Shafei, A. I.; Wise, R. G.; Gresham, G. A.; Bronns, G.; Carpenter, T. A.; Hall, L. D.; Huang, C. L. Non-invasive magnetic resonance imaging assessment of myocardial changes and the effects of angiotensin-converting enzyme inhibition in diabetic rats. *J. Physiol.* **538:**541–553; 2002.
[44] Vanhoutte, P. M.; Miller, V. M. Heterogeneity of endothelium-dependent responses in mammalian blood vessels. *J. Cardiovasc. Pharmacol.* **7:**S12–S23; 1985.
[45] Shi, Y.; Ku, D. D.; Man, R. Y.; Vanhoutte, P. M. Augmented endothelium-derived hyperpolarizing factor-mediated relaxations attenuate endothelial dysfunction in femoral and mesenteric, but not in carotid arteries from type I diabetic rats. *J. Pharmacol. Exp. Ther.* **318:**276–281; 2006.
[46] Heygate, K. M.; Lawrence, I. G.; Bennett, M. A.; Thurston, H. Impaired endothelium-dependent relaxation in isolated resistance arteries of spontaneously diabetic rats. *Br. J. Pharmacol.* **116:**3251–3259; 1995.
[47] Leo, C. H.; Hart, J. L.; Woodman, O. L. Impairment of both nitric oxide-mediated and EDHF-type relaxation in small mesenteric arteries from rats with streptozotocin-induced diabetes. *Br. J. Pharmacol.* **162:**365–377; 2011.
[48] Zanetti, M.; Barazzoni, R.; Stebel, M.; Roder, E.; Biolo, G.; Baralle, F. E.; Cattin, L.; Guarnieri, G. Dysregulation of the endothelial nitric oxide synthase-soluble guanylate cyclase pathway is normalized by insulin in the aorta of diabetic rat. *Atherosclerosis* **181:**69–73; 2005.
[49] Chen, Z.; Bakhshi, F. R.; Shajahan, A. N.; Sharma, T.; Mao, M.; Trane, A.; Bernatchez, P.; van Nieuw Amerongen, G. P.; Bonini, M. G.; Skidgel, R. A.; Malik, A. B.; Minshall, R. D. Nitric oxide-dependent Src activation and resultant caveolin-1 phosphorylation promote eNOS/caveolin-1 binding and eNOS inhibition. *Mol. Biol. Cell* **23:**1388–1398; 2012.

[50] Tschudi, M. R.; Mesaros, S.; Lüscher, T. F.; Malinski, T. Direct in situ measurement of nitric oxide in mesenteric resistance arteries. Increased decomposition by superoxide in hypertension. *Hypertension* **27:**32–35; 1996.
[51] Zielonka, J.; Kalyanaraman, B. Hydroethidine- and MitoSOX-derived red fluorescence is not a reliable indicator of intracellular superoxide formation: another inconvenient truth. *Free Radic. Biol. Med* **48:**983–1001; 2010.
[52] Liu, S.; Ma, X.; Gong, M.; Shi, L.; Lincoln, T.; Wang, S. Glucose down-regulation of cGMP-dependent protein kinase I expression in vascular smooth muscle cells involves NAD(P)H oxidase-derived reactive oxygen species. *Free Radic. Biol. Med* **42:**852–863; 2007.
[53] Laureen, J. B.; Somers, M.; Kurz, S.; McCann, L.; Warnholtz, A.; Freeman, B. A.; Tarpey, M.; Fukai, T.; Harrison, D. G. Endothelial regulation of vasomotion in apoE-deficient mice: implications for interactions between peroxynitrite and tetrahydrobiopterin. *Circulation* **103:**1282–1288; 2001.
[54] Makino, A.; Kamata, K. Elevated plasma endothelin-1 level in streptozotocin-induced diabetic rats and responsiveness of the mesenteric arterial bed to endothelin-1. *Br. J. Pharmacol* **123:**1065–1072; 1998.
[55] Romero, M.; Jiménez, R.; Sánchez, M.; López-Sepúlveda, R.; Zarzuelo, A.; Tamargo, J.; Pérez-Vizcaíno, F.; Duarte, J. Vascular superoxide production by endothelin-1 requires Src non receptor protein tyrosine kinase and MAPK activation. *Atherosclerosis* **212:**78–85; 2010.